

Relation between equilibrium quantum phase transitions and dynamical quantum phase transitions in two-band systems

Yumeng Zeng^{1,2} and Shu Chen^{1,2,*}

¹*Beijing National Laboratory for Condensed Matter Physics,*

Institute of Physics, Chinese Academy of Sciences, Beijing 100190, China

²*School of Physical Sciences, University of Chinese Academy of Sciences, Beijing 100049, China*
(Dated: November 12, 2024)

The dynamical quantum phase transition (DQPT) is an important concept in non-equilibrium critical phenomena, however, its relation to the equilibrium quantum phase transition (EQPT) remains obscure. Substantial evidences have suggested that quenching across the underlying equilibrium phase boundary is neither a sufficient nor a necessary condition for the existence of the DQPT. In this work, we give a necessary and sufficient condition for the occurrence of DQPTs in two-band systems by introducing the quench fidelity, which is defined as the fidelity between the ground state wavefunctions of the pre-quench and post-quench Hamiltonian, and elaborate it by taking one-dimensional anisotropic XY model as an example. The relation between EQPTs and DQPTs is analyzed in detail in terms of the quench fidelity.

I. INTRODUCTION

The equilibrium quantum phase transition (EQPT) is caused by the quantum fluctuations and controlled by the parameters of the Hamiltonian of the system¹. The existence of the EQPT reveals that quantum systems with parameters in different equilibrium quantum phases have distinct ground-state properties^{2,3}. The fidelity, which is the module of the overlap of two ground states of Hamiltonians with different parameter values, is widely used to describe the non-analytic changes of the properties of ground states around EQPT points²⁻¹⁵. Using $\gamma = (\gamma_1, \gamma_2, \dots)$ to denote phase-driving parameters of the quantum system, the fidelity can be formulated as

$$\mathcal{F}(\gamma, \tilde{\gamma}) = |\langle \psi^0(\gamma) | \psi^0(\tilde{\gamma}) \rangle|, \quad (1)$$

where $|\psi^0(\gamma)\rangle$ denotes the ground state of the Hamiltonian $H(\gamma)$ and $\tilde{\gamma}$ represents parameters with values different from γ . A previous work has unveiled that $\mathcal{F}(\gamma, \tilde{\gamma})$ has (has not) exact zeros in the thermodynamical limit for γ and $\tilde{\gamma}$ are in different (the same) phases¹⁵. To eliminate the effect of the Anderson orthogonality catastrophe¹⁶ (OC) in the thermodynamical limit, it is natural to introduce the decay rate function given by

$$\alpha(\gamma, \tilde{\gamma}) = -\frac{1}{L} \ln \mathcal{F}(\gamma, \tilde{\gamma}), \quad (2)$$

where L is the size of the system. Fixing the value of γ and changing the value of $\tilde{\gamma}$, $\alpha(\tilde{\gamma})$ will exhibit non-analytical behavior in the thermodynamical limit at EQPT points. Thus the decay rate function $\alpha(\tilde{\gamma})$ is a valid tool to probe the EQPT.

Since the dynamical quantum phase transition (DQPT) was proposed more than a decade ago¹⁷, it has been widely recognized that the DQPT is closely related to the EQPT¹⁸⁻³⁰. The DQPT is a phenomenon in non-equilibrium systems which indicates that the time-evolution state evolves into an orthogonal state of the

initial state. As an analogue of the fidelity in EQPT theory, the Loschmidt echo (LE) is a key concept in DQPT theory. For an initial state $|\psi_i\rangle$ which is the ground state of the initial Hamiltonian H_i and its time evolution state $|\psi(t)\rangle = e^{-iH_f t} |\psi_i\rangle$ which is driven by a post-quench Hamiltonian H_f , the LE is defined as

$$\mathcal{L}(t) = |\langle \psi_i | \psi(t) \rangle|^2, \quad (3)$$

which represents the return probability of the time-evolution state to the initial state. Similar to the fidelity at EQPT points, the LE has exact zeros at critical times when DQPTs happen^{31,32}. Similarly, to remove the effect of system size properly, the rate function of the LE is introduced as

$$\lambda(t) = -\frac{1}{L} \ln \mathcal{L}(t), \quad (4)$$

where L is the size of the system. Evidently, the exact zero of the LE $\mathcal{L}(t)$ can give rise to the singularity of the rate function $\lambda(t)$. Therefore, DQPTs can be characterized by non-analytic behaviors of the rate function $\lambda(t)$ of the LE in the real-time evolution.

In previous works^{17-19,26}, it is commonly believed that the condition for the occurrence of DQPTs is consistent with EQPTs, i.e., if the phase-driving parameters are suddenly quenched across the underlying equilibrium phase boundary at the initial time $t = 0$, DQPTs will arise at certain critical times. In noninteracting topological systems, it is clear that DQPTs have to occur if the topological number changes under the quench in 1D systems^{21,33}, while the occurrence of DQPTs are related to the change in the absolute value of the Chern number in 2D systems²³. These types of DQPTs are robust and are therefore termed topologically protected. However, it has been discovered that certain particular models do have DQPTs even for pre-quench and post-quench parameters in the same equilibrium phase, which are termed *accidental* DQPTs^{21,27,34,35}. In fact, quenching across the underlying equilibrium phase boundary is neither a

sufficient nor a necessary condition for the existence of the DQPT^{36–46}. It means that DQPT may not happen even quenching across the underlying EQPT point. So here comes the question: is there an intrinsic relation between EQPTs and DQPTs?

In this paper, we expose the relation between EQPTs and DQPTs in two-band systems from a new perspective by introducing a concept of the quench fidelity. In terms of the quench fidelity, we give a universal necessary and sufficient condition for the occurrence of DQPTs. Then, we demonstrate our theory by taking the XY model as a concrete example and calculating it in detail. Through analysis of the distribution of values of each k -mode of the quench fidelity, we also propose a sufficient condition for the occurrence of DQPTs. At last, we discuss the relationship between quenching across the equilibrium phase transition point and the existence of DQPTs.

II. THE QUENCH FIDELITY

In order to discuss DQPTs and EQPTs in the same framework, we shall introduce the definition of the quench fidelity and reveal its role in connecting EQPTs and DQPTs.

To start with, we consider a general two-band system of which the Hamiltonian in momentum space can be expressed as

$$H_k(\gamma) = \mathbf{d}_k(\gamma) \cdot \boldsymbol{\sigma} + d_{0,k}(\gamma)\mathbb{I}, \quad (5)$$

where $H_k(\gamma)$ is the Hamiltonian of k -mode with momentum k ; $\boldsymbol{\sigma} = (\sigma_x, \sigma_y, \sigma_z)$ are Pauli matrices; $\mathbf{d}_k(\gamma) = (d_{x,k}(\gamma), d_{y,k}(\gamma), d_{z,k}(\gamma))$ and $d_{0,k}(\gamma)$ are corresponding vector components of $H_k(\gamma)$; and \mathbb{I} denotes the unit matrix. Choosing $H_i = H(\gamma_i)$ as the initial Hamiltonian, where γ_i is the pre-quench parameter. At time $t = 0$, suddenly quenching the value of γ from γ_i to γ_f , i.e., $\gamma = \gamma_i\Theta(-t) + \gamma_f\Theta(t)$. Then the LE of the system which is evolved under the post-quench Hamiltonian $H_f = H(\gamma_f)$ can be represented as

$$\mathcal{L}(t) = \prod_k \mathcal{L}_k(t) = \prod_k |\langle \psi_{i,k}^0 | e^{-iH_f k t} | \psi_{i,k}^0 \rangle|^2, \quad (6)$$

where $H_{f,k}$ is the Hamiltonian of k -mode with parameter γ_f , and $|\psi_{i,k}^0\rangle$ is the ground state of the pre-quench Hamiltonian $H_{i,k}$ of k -mode with parameter γ_i . Then we have the k -mode of the LE:

$$\mathcal{L}_k(t) = 1 - [1 - (\hat{\mathbf{d}}_k(\gamma_i) \cdot \hat{\mathbf{d}}_k(\gamma_f))^2] \sin^2(|\mathbf{d}_k(\gamma_f)|t), \quad (7)$$

where $\hat{\mathbf{d}}_k(\gamma_{i/f}) = \mathbf{d}_k(\gamma_{i/f})/|\mathbf{d}_k(\gamma_{i/f})|$ and $|\mathbf{d}_k(\gamma_{i/f})| = \sqrt{d_{x,k}^2(\gamma_{i/f}) + d_{y,k}^2(\gamma_{i/f}) + d_{z,k}^2(\gamma_{i/f})}$.

The occurrence of the DQPT requires at least one k_c -mode of the LE equals to 0, i.e., $\mathcal{L}_{k_c}(t_{c,n}) = 0$, where n is a positive integer and $t_{c,n} = (2n - 1)\pi/(2|\mathbf{d}_{k_c}(\gamma_f)|)$ are critical times when DQPTs happen³². Since

$\sin^2(|\mathbf{d}_{k_c}(\gamma_f)|t_{c,n})$ always equals to 1, it is easy to get $\mathcal{L}_{k_c}(t_{c,n}) = (\hat{\mathbf{d}}_{k_c}(\gamma_i) \cdot \hat{\mathbf{d}}_{k_c}(\gamma_f))^2$. Evidently, $\mathcal{L}_{k_c}(t_{c,n}) = 0$ is fulfilled if and only if $\hat{\mathbf{d}}_{k_c}(\gamma_i) \cdot \hat{\mathbf{d}}_{k_c}(\gamma_f) = 0$, i.e., $\hat{\mathbf{d}}_{k_c}(\gamma_i)$ and $\hat{\mathbf{d}}_{k_c}(\gamma_f)$ are perpendicular on the Bloch sphere²¹. Whereas what we care about is whether such a k_c exists for various values of γ_i and γ_f , we take no account of values of critical times $t_{c,n}$ when \mathcal{L}_{k_c} equals to zero, and investigate properties of $\bar{\mathcal{L}}_k = \mathcal{L}_k(\pi/(2|\mathbf{d}_k(\gamma_f)|))$ which is the minimum of $\mathcal{L}_k(t)$ in time instead of $\mathcal{L}_k(t)$. According to Eq. (7), it is easy to get

$$\bar{\mathcal{L}}_k = (\hat{\mathbf{d}}_k(\gamma_i) \cdot \hat{\mathbf{d}}_k(\gamma_f))^2, \quad (8)$$

which is time independent and equals to zero only for the k_c -mode, i.e., $\bar{\mathcal{L}}_{k_c} = 0$.

Now, we introduce the definition of the quench fidelity:

$$\mathcal{F}^q = \prod_k \mathcal{F}_k^q = \prod_k |\langle \psi_{i,k}^0 | \psi_{f,k}^0 \rangle|, \quad (9)$$

where $|\psi_{i,k}^0\rangle$ and $|\psi_{f,k}^0\rangle$ are ground states of pre-quench Hamiltonian $H_{i,k}$ and post-quench Hamiltonian $H_{f,k}$, respectively. Comparing Eq. (9) with Eq. (1), the difference is that the two parameters of the quench fidelity are fixed to pre-quench parameter and post-quench parameter, respectively. Then we have the k -mode of the quench fidelity:

$$\mathcal{F}_k^q = \sqrt{\frac{1}{2}(1 + \hat{\mathbf{d}}_k(\gamma_i) \cdot \hat{\mathbf{d}}_k(\gamma_f))}. \quad (10)$$

For the case γ_i and γ_f are in different equilibrium phases, \mathcal{F}^q has at least one k_0 -mode that fulfills $\mathcal{F}_{k_0}^q = 0$, thus there exists at least one k_0 -mode that fulfills $\hat{\mathbf{d}}_{k_0}(\gamma_i) \cdot \hat{\mathbf{d}}_{k_0}(\gamma_f) = -1$, i.e., $\hat{\mathbf{d}}_{k_0}(\gamma_i)$ and $\hat{\mathbf{d}}_{k_0}(\gamma_f)$ are antiparallel on the Bloch sphere.

Comparing Eq. (10) with Eq. (8), it is straightforward to get

$$\bar{\mathcal{L}}_k = [2(\mathcal{F}_k^q)^2 - 1]^2. \quad (11)$$

Eq. (11) implies that the k_c -mode of the LE which satisfies $\bar{\mathcal{L}}_{k_c} = 0$ corresponds to the k_c -mode of \mathcal{F}^q which satisfies $\mathcal{F}_{k_c}^q = \sqrt{2}/2$. Therefore, a necessary and sufficient condition for the occurrence of DQPTs is the quench fidelity of the pre-quench system and the post-quench system has at least a k_c -mode which satisfies $\mathcal{F}_{k_c}^q = \sqrt{2}/2$. For a two-band system, if $d_{0,k_c}(\gamma_f) = 0$, then

$$H_{k_c}(\gamma_f) |\psi_{k_c}^0(\gamma_i)\rangle \propto |\psi_{k_c}^1(\gamma_i)\rangle$$

can be derived from $\mathcal{F}_{k_c}^q = \sqrt{2}/2$, where $|\psi_{k_c}^1(\gamma_i)\rangle$ is the first excited state of $H_{k_c}(\gamma_i)$. It implies $\langle \psi_{k_c}^0(\gamma_i) | H_{k_c}(\gamma_f) | \psi_{k_c}^0(\gamma_i) \rangle = 0$. And further $\langle \psi_{k_c}^0(\gamma_i) | H_{k_c}^2(\gamma_f) | \psi_{k_c}^0(\gamma_i) \rangle = |\mathbf{d}_{k_c}(\gamma_f)|^2$ can be derived. If $d_{0,k_c}(\gamma_i)$ is also equal to 0, then $H_{k_c}(\gamma_i)$ anti-commutes with $H_{k_c}(\gamma_f)$, i.e.,

$$\{H_{k_c}(\gamma_i), H_{k_c}(\gamma_f)\} = 0.$$

The detailed derivation of these formulas is given in Appendix A.

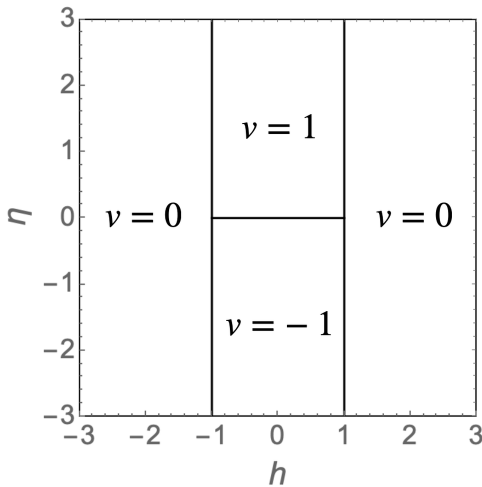


Figure 1: The equilibrium phase diagram of the XY model. ν is the winding number in each phase.

III. THE MODEL AND RESULTS

To make our theory more concrete, now we consider exploring the quenching property of a well-known model. Due to the exceptional dynamical phase transition phenomena in the one-dimensional anisotropic XY model^{34,36}, we choose it as an example system to elaborate the relation between EQPTs and DQPTs.

The Hamiltonian of the one-dimensional spin- $\frac{1}{2}$ anisotropic XY model in a transverse field is described as⁴⁷⁻⁴⁹

$$H = - \sum_{l=1}^L \left(\frac{1+\eta}{2} \sigma_l^x \sigma_{l+1}^x + \frac{1-\eta}{2} \sigma_l^y \sigma_{l+1}^y + h \sigma_l^z \right), \quad (12)$$

where η is the anisotropy parameter, h denotes the

strength of the transverse field, and the periodic boundary condition $\sigma_{L+1}^{x/y} = \sigma_1^{x/y}$ is applied. Using the Jordan-Wigner transformation, this model can be mapped to the spinless fermion representation as

$$H = - \sum_{l=1}^L (c_l^\dagger c_{l+1} + \eta c_l^\dagger c_{l+1}^\dagger + \text{H.c.}) - \sum_{l=1}^L h (2c_l^\dagger c_l - 1). \quad (13)$$

Here we adopt periodic boundary condition $c_{L+1} = c_1$ and take even L . After the Fourier transformation $c_l^\dagger = \frac{1}{\sqrt{L}} \sum_k e^{ikl} c_k^\dagger$, the Hamiltonian in the momentum space can be written as

$$H = \sum_{k \in \mathcal{K}} \Psi_k^\dagger H_k \Psi_k - 2(h+1)c_0^\dagger c_0 - 2(h-1)c_\pi^\dagger c_\pi + 2h, \quad (14)$$

where $\Psi_k = (c_k, c_{-k}^\dagger)^T$, $\mathcal{K} = \{ \frac{2\pi m}{L} \mid m = 1, 2, \dots, \frac{L-1}{2} \}$, and H_k takes the form of Eq. (5) with the vector components expressed as

$$d_{x,k} = -2h - 2\cos k, \quad (15)$$

$$d_{y,k} = -2\eta \sin k, \quad (16)$$

and $d_{z,k} = d_{0,k} = 0$. The equilibrium phase diagram of the XY model are shown in Fig. 1. There are three equilibrium phase boundaries: The critical line $h = -1$ where energy gap close at $k = 0$, the critical line $h = 1$ where energy gap close at $k = \pi$, and the critical line $\eta = 0$ for $-1 < h < 1$ where energy gap close at $k = \pm \arccos(-h)$. The winding number ν is defined by $\nu = \frac{1}{2\pi} \int_{-\pi}^{\pi} dk \frac{d_{x,k} \partial_k d_{y,k} - d_{y,k} \partial_k d_{x,k}}{d_{x,k}^2 + d_{y,k}^2}$.

Choosing (h, η) as quench parameters, and quenching them from (h_i, η_i) to (h_f, η_f) at time $t = 0$, then we get

$$\bar{\mathcal{L}}_k = \frac{[(h_i + \cos k)(h_f + \cos k) + \eta_i \eta_f \sin^2 k]^2}{[(h_i + \cos k)^2 + \eta_i^2 \sin^2 k][(h_f + \cos k)^2 + \eta_f^2 \sin^2 k]}, \quad (17)$$

$$\mathcal{F}_k^q = \sqrt{\frac{(h_i + \cos k)(h_f + \cos k) + \eta_i \eta_f \sin^2 k}{2\sqrt{[(h_i + \cos k)^2 + \eta_i^2 \sin^2 k][(h_f + \cos k)^2 + \eta_f^2 \sin^2 k]}}} + \frac{1}{2}. \quad (18)$$

To exhibit the distribution of post-quench parameters which possess $\bar{\mathcal{L}}_k = 0$ for $h_i = -2$ and $\eta_i = 0.8$, we plot Fig. 2(a) where cyan solid lines are post-quench parameters which possess $\bar{\mathcal{L}}_k = 0$ with $k \in \{2\pi m/L \mid m = 1, 2, \dots, (L-1)/2\}$ from lighter to darker, here $L = 30$. Each post-quench parameter point has as many k_c -modes which satisfy $\bar{\mathcal{L}}_{k_c} = 0$ as the number of cyan solid lines that pass through it. According

to the number n_{k_c} of k_c -modes owned by the post-quench parameter points, we plot the dynamical phase diagram of DQPTs of the XY model in the thermodynamic limit for $h_i = -2$ and $\eta_i = 0.8$ as shown in Fig. 2(b). Compared with Fig. 1(a), the two additional dashed lines in Fig. 2(b) demonstrate differences between dynamical phase boundaries and equilibrium phase boundaries. Obviously, DQPTs will occur when post-quench param-

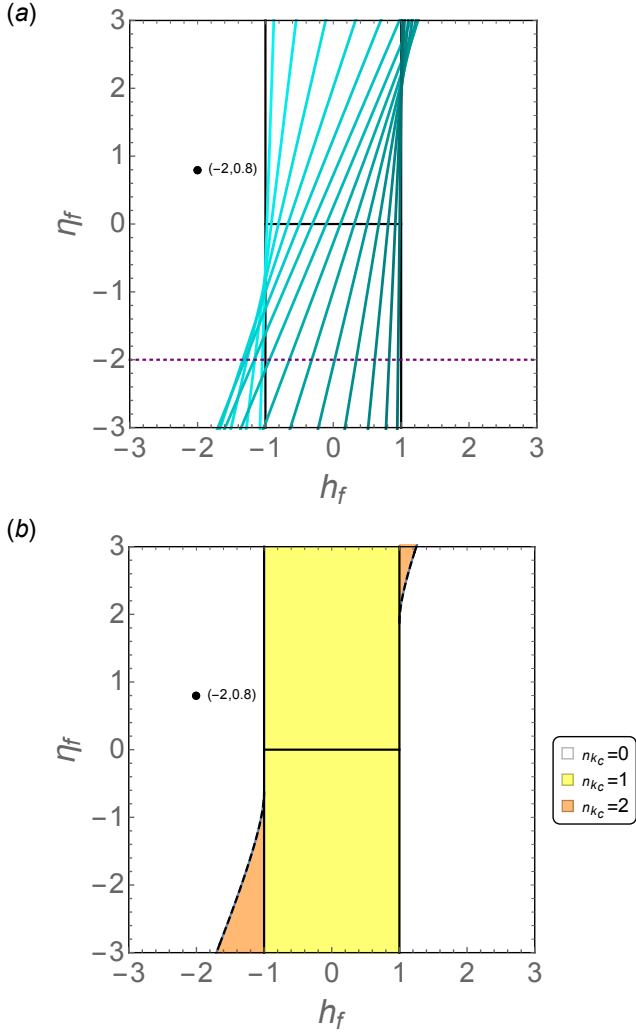


Figure 2: (a) The distribution of k_c -modes $\bar{\mathcal{L}}_{k_c}$ in the post-quench parameter space spanned by h_f and η_f . The cyan solid lines are post-quench parameters which possess $\bar{\mathcal{L}}_k = 0$ with $k \in \{2\pi m/L \mid m = 1, 2, \dots, (L-1)/2\}$ from lighter to darker. The purple dotted line denotes $\eta_f = -2$. The black dot denotes point $(-2, 0.8)$. Here $L = 30$. (b) The dynamical phase diagram of DQPTs of the XY model with different numbers n_{k_c} of the LE. DQPTs will occur when post-quench parameters are in yellow and orange regions. Here $h_i = -2$ and $\eta_i = 0.8$.

ters are in yellow and orange regions in Fig. 2(b). Since k_c -modes may exist for post-quench parameters and pre-quench parameters being in the same phase, even quenching within the same equilibrium phase may also lead to the occurrence of DQPTs.

Setting $\eta_f = -2$, we plot the density graphic of $\bar{\mathcal{L}}_k$ versus k and h_f in Fig. 3(a). The cyan solid line represents $\bar{\mathcal{L}}_k = 0$. As seen from Fig. 3(a), whenever post-quench parameters across dynamical phase boundaries of DQPTs as depicted in Fig. 2(b), there is a change in the number of k_c -modes but no abrupt change of $\bar{\mathcal{L}}_k$. Fig. 3(b) and 3(c) exhibit images of the rate function

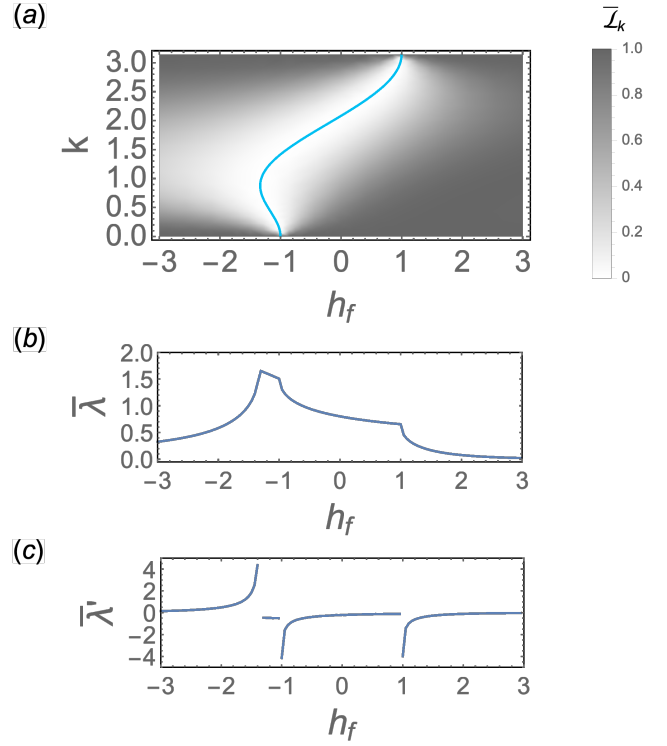


Figure 3: (a) The density graphic of $\bar{\mathcal{L}}_k$ versus k and h_f . The cyan solid line represents $\bar{\mathcal{L}}_k = 0$. (b) The image of the rate function $\bar{\lambda}$ versus h_f . (c) The image of the derivative of the rate function $\bar{\lambda}'$ versus h_f . Here $h_i = -2$, $\eta_i = 0.8$, and $\eta_f = -2$.

$\bar{\lambda} = -\frac{1}{L} \sum_k \ln \bar{\mathcal{L}}_k$ and its derivative $\bar{\lambda}'$ with respect to h_f . The rate function $\bar{\lambda}$ exhibits non-analyticity at all three dynamical phase boundaries. The derivative $\bar{\lambda}'$ becomes divergent when approaching a dynamical phase boundary from a region with less number of k_c -modes to a region with more number of k_c -modes, while it keeps finite at the other side. We cannot distinguish the additional phase boundary of DQPTs from the two boundaries that coincides with equilibrium phase boundaries through the image of the rate function, because the abrupt changes of k -modes \mathcal{F}_k^q with $k = 0$ and $k = \pi$ from 1 to 0 or from 0 to 1 at the two equilibrium phase boundaries are unchanged for $\bar{\mathcal{L}}_k$ according to Eq. (11). There is only a change of the number of k_c -modes but no abrupt change of $\bar{\mathcal{L}}_k$ at all three boundaries.

For consistency, we call k -modes satisfying $\mathcal{F}_k^q = 0$ as k_0 -modes and call k -modes satisfying $\mathcal{F}_k^q = 1$ as k_1 -modes in the following. To exhibit how k -modes \mathcal{F}_k^q change at equilibrium phase boundaries, we display the distribution of k_0 -modes $\mathcal{F}_{k_0}^q$ and k_1 -modes $\mathcal{F}_{k_1}^q$ in the space of post-quench parameter with the fixed pre-quench parameters $h_i = -2$ and $\eta_i = 0.8$ in Fig. 4(a). The red dashed lines and green dotted lines depict post-quench parameters which possess $\mathcal{F}_k^q = 1$ and $\mathcal{F}_k^q = 0$ with $k \in \{2\pi m/L \mid m = 1, 2, \dots, (L-1)/2\}$ from lighter to

darker, respectively. Here $L = 30$. In addition, for $k = 0$, we have $\mathcal{F}_0^q = 1$ for $h_f < -1$, and $\mathcal{F}_0^q = 0$ for $h_f > -1$. For $k = \pi$, we have $\mathcal{F}_\pi^q = 1$ for $h_f < 1$, and $\mathcal{F}_\pi^q = 0$ for $h_f > 1$. It is evident that there are only k_1 -modes but no k_0 -modes for $h_f < -1$, there are both k_0 -modes and k_1 -modes for $-1 < h_f < 1$, and there are only k_0 -modes but no k_1 -modes for $h_f > 1$. From Fig. 4(a), we can conclude that each point on equilibrium phase boundaries corresponds to a k -mode \mathcal{F}_k^q whose value will suddenly change at that point and smoothly change everywhere else. Setting $h_i = -2$ and $\eta_i = 0.8$, we divide the post-quench parameter space in the thermodynamic limit into four kinds of regions as shown in Fig. 4(b) and 4(c), according to the number n_{k_0} of k_0 -modes which satisfy $\mathcal{F}_{k_0} = 0$ and the number n_{k_1} of k_1 -modes which satisfy $\mathcal{F}_{k_1} = 1$, respectively. Although Fig. 4(b) and 4(c) are a little different from Fig. 1, the overlapping boundaries of Fig. 4(b) and 4(c) match exactly the equilibrium phase boundaries of Fig. 1. It implies both n_{k_0} and n_{k_1} change at equilibrium phase boundaries. Comparing Fig. 4(b) with Fig. 1, we find that Fig. 4(b) has two extra dashed lines across which there will appear more or less k_0 -modes, whereas abrupt change in each \mathcal{F}_k^q only occurs at equilibrium phase boundaries and not here, which we will demonstrate later. Besides, positions of these two extra dashed lines depend on the value of h_i and η_i and thus are not robust.

Setting $\eta_f = -2$, we plot the density graphic of \mathcal{F}_k^q versus k and h_f in Fig. 5(a). The red dashed lines represent $\mathcal{F}_k^q = 1$, and the green dotted lines represent $\mathcal{F}_k^q = 0$. As seen from Fig. 5(a), when the post-quench parameter across the equilibrium phase boundaries $h_f = -1$ and $h_f = 1$, there is a k -mode \mathcal{F}_k^q abruptly drops from 1 to 0. When the parameter across the extra boundary in Fig. 4(b), there is only a change in the number of k_0 -modes without any abrupt change in each \mathcal{F}_k^q . Fig. 5(b) and 5(c) exhibit images of the decay rate function of the quench fidelity $\alpha^q = -\frac{1}{L} \ln \mathcal{F}^q$ and its derivative $\alpha^{q'}$ with respect to h_f . The decay rate function exhibits non-analyticity at all three boundaries. Nonetheless, the derivative $\alpha^{q'}$ is divergent around the two equilibrium phase boundaries but is finite at one side of the additional boundary. It is because there is only a change of the number of k_0 -modes but no abrupt change of \mathcal{F}_k^q at the extra boundary, while both of them change at equilibrium phase boundaries. As a result, the behavior of the derivative $\alpha^{q'}$ can distinguish equilibrium phase boundaries from extra boundaries.

Next we explore the relation between \mathcal{F}_k^q and $\bar{\mathcal{L}}_k$ of the XY model. According to Eq. (11), we plot the image of $\bar{\mathcal{L}}_k$ versus \mathcal{F}_k^q in Fig. 6(a). It demonstrates that $\bar{\mathcal{L}}_k$ must undergo a zero value as long as \mathcal{F}_k^q goes from 0 to 1. Because \mathcal{F}_k^q is a continuous function of k , if the fidelity \mathcal{F}^q has a k_0 -mode which satisfies $\mathcal{F}_{k_0}^q = 0$ and a k_1 -mode which satisfies $\mathcal{F}_{k_1}^q = 1$, then \mathcal{F}^q must have at least a k_c -mode between k_0 and k_1 which satisfies $\mathcal{F}_{k_c}^q = \sqrt{2}/2$ so that $\bar{\mathcal{L}}_{k_c} = 0$. As a consequence, a sufficient condition for the occurrence of DQPTs is the quench fidelity \mathcal{F}^q has

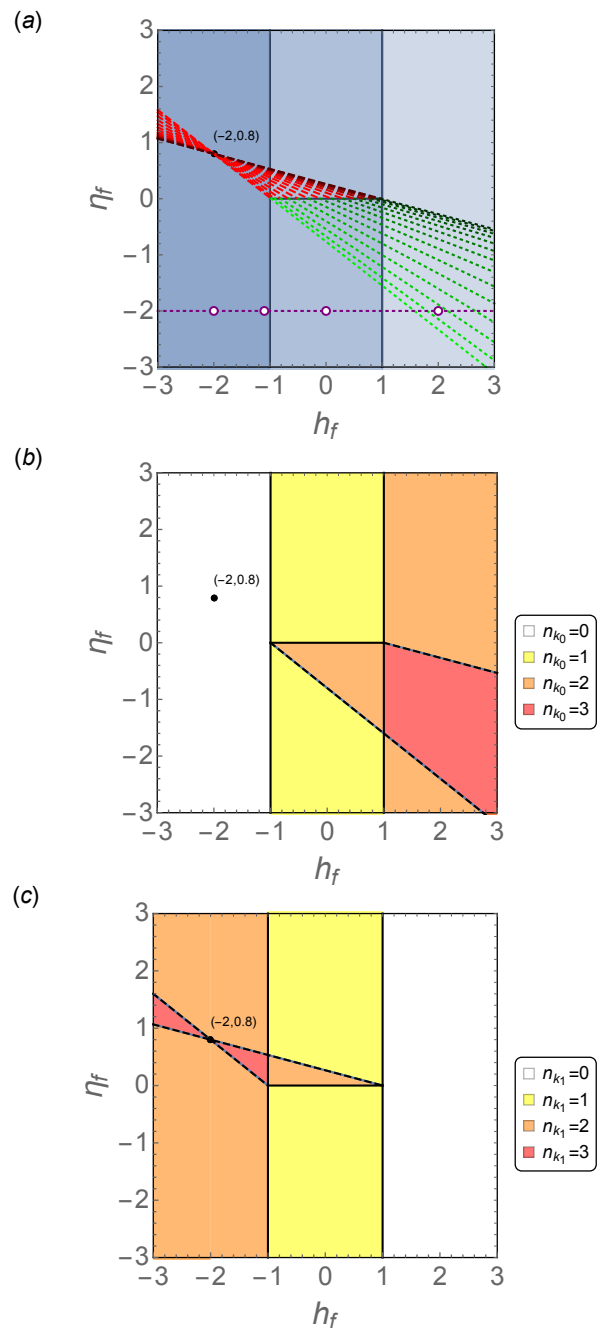


Figure 4: (a) The distribution of k_0 -modes $\mathcal{F}_{k_0}^q$ and k_1 -modes $\mathcal{F}_{k_1}^q$ in the post-quench parameter space spanned by h_f and η_f . The red dashed lines and green dotted lines depict post-quench parameters which possess $\mathcal{F}_k^q = 1$ and $\mathcal{F}_k^q = 0$ with $k \in \{2\pi m/L \mid m = 1, 2, \dots, (L-1)/2\}$ from lighter to darker, respectively. The post-quench parameters in dark blue region $h_f < -1$ possess both $\mathcal{F}_0^q = 1$ and $\mathcal{F}_\pi^q = 1$. The post-quench parameters in light blue region $-1 < h_f < 1$ possess $\mathcal{F}_0^q = 0$ and $\mathcal{F}_\pi^q = 1$. The post-quench parameters in faint blue region $h_f > 1$ possess both $\mathcal{F}_0^q = 0$ and $\mathcal{F}_\pi^q = 0$. The purple dotted line denotes $\eta_f = -2$. The black dot denotes point $(-2, 0.8)$. Here $L = 30$. (b) and (c) are regions with different values of n_{k_0} and n_{k_1} , respectively. Solid black lines are original equilibrium phase boundaries, and dashed black lines are additional boundaries. Here $h_i = -2$ and $\eta_i = 0.8$.

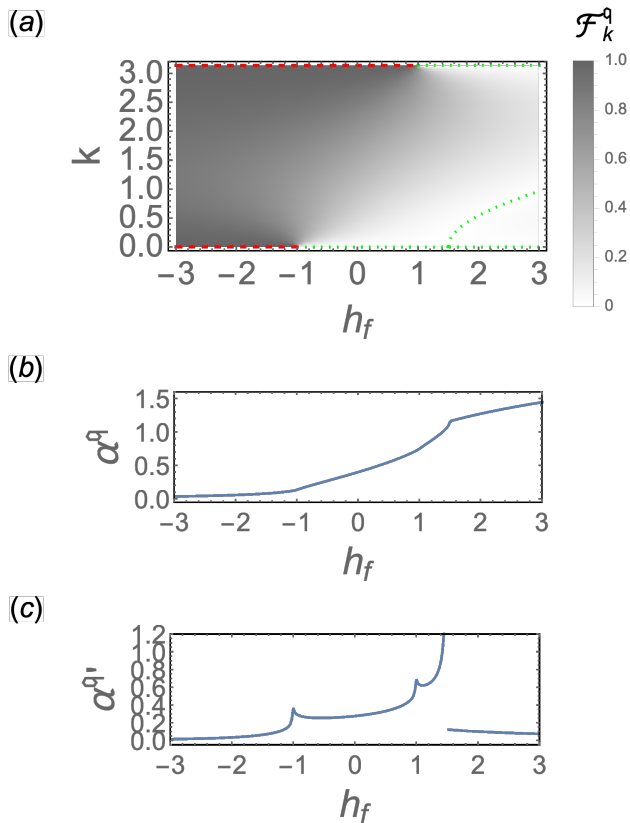


Figure 5: (a) The density graphic of \mathcal{F}_k^q versus k and h_f . The red dashed lines and green dotted lines represent $\mathcal{F}_k^q = 1$ and $\mathcal{F}_k^q = 0$, respectively. (b) The image of the decay rate function α^q versus h_f . (c) The image of the derivative of the decay rate function $\alpha^{q'}$ versus h_f . Here $h_i = -2$, $\eta_i = 0.8$ and $\eta_f = -2$.

at least a k_0 -mode and a k_1 -mode simultaneously. To make it more intuitional, we take the four post-quench parameter points denoted by purple circle on the purple dashed line in Fig. 4(a) as cases, and plot images of \mathcal{F}_k^q and $\bar{\mathcal{L}}_k$ versus k in Fig. 6 (b)-(e). The dark blue and light blue solid lines represent \mathcal{F}_k^q and $\bar{\mathcal{L}}_k$, respectively. The blue horizontal dashed lines represent $\sqrt{2}/2$, and the black vertical dashed lines denote corresponding k_c . Setting $h_i = -2$ and $\eta_i = 0.8$, Fig. 6(b) and 6(e) show that the quench fidelity only have k_1 -modes or k_0 -modes and the images of \mathcal{F}_k^q do not cross the dashed line, thus there is no k_c -mode satisfies $\bar{\mathcal{L}}_{k_c} = 0$, which means no DQPT will happen. Fig. 6(d) shows the quench fidelity has both a k_0 -mode and a k_1 -mode, and the image of \mathcal{F}_k^q certainly cross the horizontal dashed line, thus $\bar{\mathcal{L}}_k$ becomes 0 at the cross point k_c and DQPTs can occur. Besides, even if the quench fidelity only have k_1 -modes and have no k_0 -mode, the image of \mathcal{F}_k^q can still cross the dashed line, which leads to the occurrence of DQPTs as shown in Fig. 6(c). This is consistent with Fig. 2(b) and Fig. 4(a): The quench fidelity has both k_0 -modes and k_1 -modes for $-1 < h_f < 1$, thus DQPTs must occur when post-quench

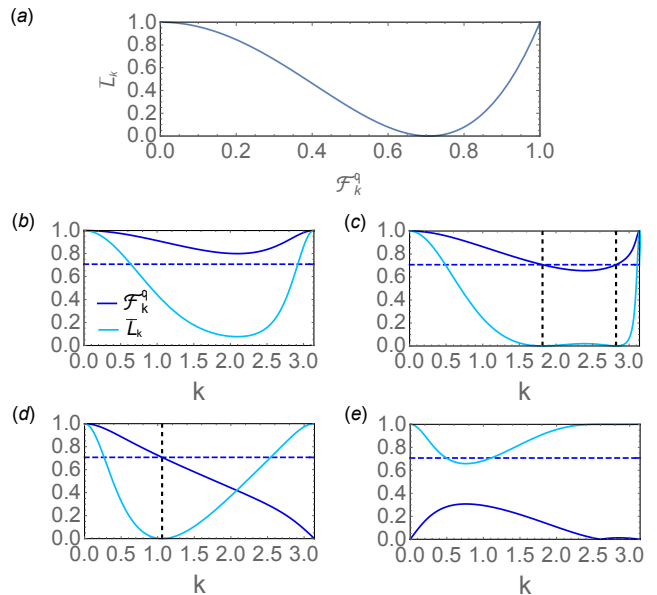


Figure 6: (a) The image of $\bar{\mathcal{L}}_k$ versus \mathcal{F}_k^q . (b)-(e) are images of \mathcal{F}_k^q and $\bar{\mathcal{L}}_k$ versus k . The dark blue solid lines are \mathcal{F}_k^q . The light blue solid lines are $\bar{\mathcal{L}}_k$. The blue horizontal dashed lines represent $\sqrt{2}/2$. The black vertical dashed lines denote corresponding k_c . Post-quench parameters are: (b) $h_f = -2$, $\eta_f = -2$; (c) $h_f = -1.1$, $\eta_f = -2$; (d) $h_f = 0$, $\eta_f = -2$; (e) $h_f = 2$, $\eta_f = -2$. Here $h_i = -2$ and $\eta_i = 0.8$.

parameters are in this region. While for $h_f < -1$ and $h_f > 1$, the quench fidelity has either only k_1 -modes or only k_0 -modes, thus DQPTs may or may not occur in these regions. In a nutshell, since the necessary and sufficient condition for DQPTs is the quench fidelity of the pre-quench system and the post-quench system has at least a k_c -mode which satisfies $\mathcal{F}_{k_c}^q = \sqrt{2}/2$, whereas the necessary and sufficient condition for crossing the EQPT point is the quench fidelity has at least a k_0 -mode which satisfies $\mathcal{F}_{k_0}^q = 0$, crossing the EQPT point is neither sufficient nor necessary for the occurrence of DQPTs.

IV. CONCLUSION AND DISCUSSION

In summary, we proposed the concept of the quench fidelity and applied it to unveil the relation between EQPTs and DQPTs from a new perspective. By using $\bar{\mathcal{L}}_k$ to denote the minimum of each $\mathcal{L}_k(t)$ in time, and defining the quench fidelity \mathcal{F}^q as the module of the overlap of ground states of the Hamiltonian with pre-quench parameter and the one with post-quench parameter, we found the relation between $\bar{\mathcal{L}}_k$ and \mathcal{F}_k^q , which reveals that the occurrence of DQPTs corresponds to k_c -modes of \mathcal{F}^q which satisfy $\mathcal{F}_{k_c}^q = \sqrt{2}/2$. Therefore, a necessary and sufficient condition for the existence of DQPTs is the quench fidelity of the pre-quench system and the post-quench system has at least a k_c -mode which satisfies

$$\mathcal{F}_{k_c}^q = \sqrt{2}/2.$$

To demonstrate our theory, we took the one-dimensional spin- $\frac{1}{2}$ anisotropic XY model as a concrete example and calculated it in detail. According to the number n_{k_c} of k_c -modes, we divided the post-quench parameter space into three kinds of regions, and thus got the dynamical phase diagram of DQPTs of the XY model for given pre-quench parameters. In comparison with the original equilibrium phase diagram, the dynamical phase diagram of XY model has two additional boundaries, which demonstrates the essential difference between EQPTs and DQPTs. According to the number n_{k_0} of k_0 -modes and the number n_{k_1} of k_1 -modes, we divided the post-quench parameter space into different regions. Although phase diagrams of k_0 -modes and k_1 -modes are a little different from the original equilibrium phase diagram, the overlapping boundaries of them match exactly the equilibrium phase boundaries, indicating that there are changes in the values of both n_{k_0} and n_{k_1} at equilibrium phase boundaries. Besides, we found that the phase diagram of k_0 -modes has two extra boundaries across which there will appear more or less k_0 -modes, whereas abrupt change in each \mathcal{F}_k^q only occurs at equilibrium phase boundaries. The discrepancy between the extra boundaries and equilibrium phase boundaries can be demonstrated by the image of the derivative of the decay rate function of the quench fidelity. Through the image of $\bar{\mathcal{L}}_k$ versus \mathcal{F}_k^q , we concluded that a sufficient condition for the occurrence of DQPTs is the quench fidelity has at least a k_0 -mode and a k_1 -mode simultaneously, whereas DQPTs may or may not occur if the quench fidelity has only k_1 -modes or only k_0 -modes. It means that quenching across the equilibrium phase point is not sufficient for the occurrence of DQPTs unless the quench fidelity owns at least a k_1 -mode, and quenching within the same equilibrium phase can also give rise to DQPTs, which accounts for the mismatch between dynamical phases and equilibrium phases.

Our work clarifies clearly the relation between EQPTs and DQPTs and provides a new insight for future study on conditions for the occurrence of DQPTs. Nonetheless, our theory is currently limited to two-band systems, and further researches on promoting it to a broader range of models are anticipated.

Acknowledgments

This work is supported by the NSFC under Grants No. 12174436, No.12474287 and No. T2121001.

Appendix A: The detailed derivation of formulas

For simplicity, here we use $|0_{i/f}\rangle$ and $|1_{i/f}\rangle$ to denote the ground state $|\psi_{k_c}^0(\gamma_{i/f})\rangle$ and the first excited state $|\psi_{k_c}^1(\gamma_{i/f})\rangle$ of $H_{i/f,k_c}$, respectively.

For a two-band system, if $d_{0,k_c}(\gamma_f) = 0$, then the eigenvalue equations of H_{f,k_c} are

$$H_{f,k_c} |0_f\rangle = -E_{f,k_c} |0_f\rangle, \quad (\text{A1})$$

$$H_{f,k_c} |1_f\rangle = E_{f,k_c} |1_f\rangle. \quad (\text{A2})$$

Here $E_{f,k_c} = |\mathbf{d}_{k_c}(\gamma_f)|$.

Since $\mathcal{F}_{k_c} = |\langle 0_i | 0_f \rangle| = \sqrt{2}/2$, we can derive

$$\begin{aligned} |\langle 1_i | 0_f \rangle| &= \sqrt{\langle 0_f | 1_i \rangle \langle 1_i | 0_f \rangle} \\ &= \sqrt{\langle 0_f | (1 - |0_i\rangle \langle 0_i|) | 0_f \rangle} \\ &= \sqrt{\langle 0_f | 0_f \rangle - \langle 0_f | 0_i \rangle \langle 0_i | 0_f \rangle} \\ &= \sqrt{1 - |\langle 0_i | 0_f \rangle|^2} \\ &= \sqrt{1 - 1/2} \\ &= \sqrt{2}/2, \end{aligned} \quad (\text{A3})$$

and

$$\begin{aligned} |\langle 0_i | 1_f \rangle| &= \sqrt{\langle 0_i | 1_f \rangle \langle 1_f | 0_i \rangle} \\ &= \sqrt{\langle 0_i | (1 - |0_f\rangle \langle 0_f|) | 0_i \rangle} \\ &= \sqrt{\langle 0_i | 0_i \rangle - \langle 0_i | 0_f \rangle \langle 0_f | 0_i \rangle} \\ &= \sqrt{1 - |\langle 0_i | 0_f \rangle|^2} \\ &= \sqrt{1 - 1/2} \\ &= \sqrt{2}/2. \end{aligned} \quad (\text{A4})$$

Assume the argument of $\langle 1_i | 0_f \rangle \langle 0_f | 0_i \rangle$ is θ , then $\langle 1_i | 0_f \rangle \langle 0_f | 0_i \rangle = e^{i\theta} |\langle 1_i | 0_f \rangle \langle 0_f | 0_i \rangle| = e^{i\theta}/2$, thus we can derive

$$\begin{aligned} H_{f,k_c} |0_i\rangle &= H_{f,k_c} (|0_f\rangle \langle 0_f| + |1_f\rangle \langle 1_f|) |0_i\rangle \\ &= H_{f,k_c} |0_f\rangle \langle 0_f| 0_i\rangle + H_{f,k_c} |1_f\rangle \langle 1_f| 0_i\rangle \\ &= -E_{f,k_c} |0_f\rangle \langle 0_f| 0_i\rangle + E_{f,k_c} |1_f\rangle \langle 1_f| 0_i\rangle \\ &= -E_{f,k_c} |0_f\rangle \langle 0_f| 0_i\rangle + E_{f,k_c} (1 - |0_f\rangle \langle 0_f|) |0_i\rangle \\ &= -E_{f,k_c} |0_f\rangle \langle 0_f| 0_i\rangle + E_{f,k_c} |0_i\rangle \\ &\quad - E_{f,k_c} |0_f\rangle \langle 0_f| 0_i\rangle \\ &= -2E_{f,k_c} |0_f\rangle \langle 0_f| 0_i\rangle + E_{f,k_c} |0_i\rangle \\ &= -2E_{f,k_c} (|0_i\rangle \langle 0_i| + |1_i\rangle \langle 1_i|) |0_f\rangle \langle 0_f| 0_i\rangle \\ &\quad + E_{f,k_c} |0_i\rangle \\ &= -2E_{f,k_c} |0_i\rangle \langle 0_i| 0_f\rangle \langle 0_f| 0_i\rangle \\ &\quad - 2E_{f,k_c} |1_i\rangle \langle 1_i| 0_f\rangle \langle 0_f| 0_i\rangle + E_{f,k_c} |0_i\rangle \\ &= -2E_{f,k_c} |0_i\rangle |\langle 0_i | 0_f \rangle|^2 - e^{i\theta} E_{f,k_c} |1_i\rangle \\ &\quad + E_{f,k_c} |0_i\rangle \\ &= -E_{f,k_c} |0_i\rangle - e^{i\theta} E_{f,k_c} |1_i\rangle + E_{f,k_c} |0_i\rangle \\ &= -e^{i\theta} E_{f,k_c} |1_i\rangle. \end{aligned} \quad (\text{A5})$$

As a result, we get $H_{f,k_c} |0_i\rangle \propto |1_i\rangle$. And it is easy to get $\langle 0_i | H_{f,k_c} |0_i\rangle = -e^{i\theta} E_{f,k_c} \langle 0_i | 1_i\rangle = 0$. In addition,

we can derive

$$\begin{aligned}
\langle 0_i | H_{f,k_c}^2 | 0_i \rangle &= \langle 0_i | H_{f,k_c}^2 (|0_f\rangle \langle 0_f| + |1_f\rangle \langle 1_f|) | 0_i \rangle \\
&= \langle 0_i | H_{f,k_c}^2 | 0_f \rangle \langle 0_f | 0_i \rangle \\
&\quad + \langle 0_i | H_{f,k_c}^2 | 1_f \rangle \langle 1_f | 0_i \rangle \\
&= E_{f,k_c}^2 \langle 0_i | 0_f \rangle \langle 0_f | 0_i \rangle \\
&\quad + E_{f,k_c}^2 \langle 0_i | 1_f \rangle \langle 1_f | 0_i \rangle \\
&= E_{f,k_c}^2 (|\langle 0_i | 0_f \rangle|^2 + |\langle 0_i | 1_f \rangle|^2) \\
&= E_{f,k_c}^2. \tag{A6}
\end{aligned}$$

In the same way, we can derive

$$\begin{aligned}
H_{f,k_c} | 1_i \rangle &= H_{f,k_c} (|0_f\rangle \langle 0_f| + |1_f\rangle \langle 1_f|) | 1_i \rangle \\
&= H_{f,k_c} | 0_f \rangle \langle 0_f | 1_i \rangle + H_{f,k_c} | 1_f \rangle \langle 1_f | 1_i \rangle \\
&= -E_{f,k_c} | 0_f \rangle \langle 0_f | 1_i \rangle + E_{f,k_c} | 1_f \rangle \langle 1_f | 1_i \rangle \\
&= -E_{f,k_c} | 0_f \rangle \langle 0_f | 1_i \rangle + E_{f,k_c} (1 - |0_f\rangle \langle 0_f|) | 1_i \rangle \\
&= -E_{f,k_c} | 0_f \rangle \langle 0_f | 1_i \rangle + E_{f,k_c} | 1_i \rangle \\
&\quad - E_{f,k_c} | 0_f \rangle \langle 0_f | 1_i \rangle \\
&= -2E_{f,k_c} | 0_f \rangle \langle 0_f | 1_i \rangle + E_{f,k_c} | 1_i \rangle \\
&= -2E_{f,k_c} (|0_i\rangle \langle 0_i| + |1_i\rangle \langle 1_i|) | 0_f \rangle \langle 0_f | 1_i \rangle \\
&\quad + E_{f,k_c} | 1_i \rangle \\
&= -2E_{f,k_c} | 0_i \rangle \langle 0_i | 0_f \rangle \langle 0_f | 1_i \rangle \\
&\quad - 2E_{f,k_c} | 1_i \rangle \langle 1_i | 0_f \rangle \langle 0_f | 1_i \rangle + E_{f,k_c} | 1_i \rangle \\
&= -2E_{f,k_c} | 0_i \rangle (\langle 1_i | 0_f \rangle \langle 0_f | 0_i \rangle)^* \\
&\quad - 2E_{f,k_c} | 1_i \rangle |\langle 1_i | 0_f \rangle|^2 + E_{f,k_c} | 1_i \rangle \\
&= -e^{-i\theta} E_{f,k_c} | 0_i \rangle - E_{f,k_c} | 1_i \rangle + E_{f,k_c} | 1_i \rangle \\
&= -e^{-i\theta} E_{f,k_c} | 0_i \rangle. \tag{A7}
\end{aligned}$$

If $d_{0,k_c}(\gamma_i)$ is also equal to 0, then the eigenvalue equations of H_{i,k_c} are

$$H_{i,k_c} | 0_f \rangle = -E_{i,k_c} | 0_i \rangle, \tag{A8}$$

$$H_{i,k_c} | 1_f \rangle = E_{i,k_c} | 1_i \rangle. \tag{A9}$$

Here $E_{i,k_c} = |\mathbf{d}_{k_c}(\gamma_i)|$. According to Eq. (A5) and Eq. (A7), we can get

$$\begin{aligned}
H_{i,k_c} H_{f,k_c} | 0_i \rangle &= -e^{i\theta} E_{f,k_c} H_{i,k_c} | 1_i \rangle \\
&= -e^{i\theta} E_{f,k_c} E_{i,k_c} | 1_i \rangle \\
&= E_{i,k_c} (-e^{i\theta} E_{f,k_c} | 1_i \rangle) \\
&= E_{i,k_c} H_{f,k_c} | 0_i \rangle \\
&= H_{f,k_c} E_{i,k_c} | 0_i \rangle \\
&= -H_{f,k_c} H_{i,k_c} | 0_i \rangle, \tag{A10}
\end{aligned}$$

and

$$\begin{aligned}
H_{i,k_c} H_{f,k_c} | 1_i \rangle &= -e^{-i\theta} E_{f,k_c} H_{i,k_c} | 0_i \rangle \\
&= e^{-i\theta} E_{f,k_c} E_{i,k_c} | 0_i \rangle \\
&= -E_{i,k_c} (-e^{-i\theta} E_{f,k_c} | 0_i \rangle) \\
&= -E_{i,k_c} H_{f,k_c} | 1_i \rangle \\
&= -H_{f,k_c} E_{i,k_c} | 1_i \rangle \\
&= -H_{f,k_c} H_{i,k_c} | 1_i \rangle. \tag{A11}
\end{aligned}$$

Because $\{|0_i\rangle, |1_i\rangle\}$ is a set of complete bases, we can draw a conclusion that

$$\{H_{i,k_c}, H_{f,k_c}\} = 0. \tag{A12}$$

* Electronic address: schen@iphy.ac.cn

¹ S. Sachdev, Quantum Phase Transitions (Cambridge University Press, Cambridge, 1999).

² P. Zanardi and N. Paunkovic, Ground state overlap and quantum phase transitions, Phys. Rev. E **74**, 031123 (2006).

³ W. L. You, Y. W. Li, and S. J. Gu, Fidelity, dynamic structure factor, and susceptibility in critical phenomena, Phys. Rev. E **76**, 022101 (2007).

⁴ P. Zanardi, M. Cozzini, and P. Giorda, Ground state fidelity and quantum phase transitions in free Fermi systems, J. Stat. Mech. (2007) L02002.

⁵ P. Buonsante and A. Vezzani, Ground-state fidelity and bipartite entanglement in the Bose-Hubbard model, Phys. Rev. Lett. **98**, 110601 (2007).

⁶ M. Cozzini, R. Ionicioiu, and P. Zanardi, Quantum fidelity and quantum phase transitions in matrix product states, Phys. Rev. B **76**, 104420 (2007)

⁷ M. Cozzini, P. Giorda, and P. Zanardi, Quantum phase transitions and quantum fidelity in free fermion graphs, Phys. Rev. B **75**, 014439 (2007)

⁸ M.-F. Yang, Ground-state fidelity in one-dimensional gapless models, Phys. Rev. B **76**, 180403(R) (2007).

⁹ H.-Q. Zhou, J.-H. Zhao, and B. Li, Fidelity approach to quantum phase transitions: Finite-size scaling for the quantum Ising model in a transverse field, J. Phys. A **41**, 492002 (2008).

¹⁰ S. Chen, L. Wang, Y. Hao, and Y. Wang, Intrinsic relation between ground-state fidelity and the characterization of a quantum phase transition, Phys. Rev. A **77**, 032111 (2008)

¹¹ M. M. Rams and B. Damski, Quantum fidelity in the thermodynamic limit, Phys. Rev. Lett. **106**, 055701 (2011).

¹² V. Mukherjee, A. Polkovnikov, and A. Dutta, Oscillating fidelity susceptibility near a quantum multicritical point, Phys. Rev. B **83**, 075118 (2011).

¹³ G. Sun, A. K. Kolezhuk, and T. Vekua, Fidelity at Berezinskii-Kosterlitz-Thouless quantum phase transitions, Phys. Rev. B **91**, 014418 (2015).

¹⁴ G. Sun, B.-B. Wei, and S.-P. Kou, Fidelity as a probe for a deconfined quantum critical point, Phys. Rev. B **100**, 064427 (2019).

¹⁵ Y. Zeng, B. Zhou, and S. Chen, Exact zeros of fidelity in finite-size systems as a signature for probing quantum phase transitions, Phys. Rev. E **109**, 064130 (2024).

¹⁶ P. W. Anderson, Infrared Catastrophe in Fermi Gases with Local Scattering Potentials, Phys. Rev. Lett. **18**, 1049

- (1967).
- ¹⁷ M. Heyl, A. Polkovnikov and S. Kehrein, dynamical quantum phase transitions in the transverse-field Ising model, *Phys. Rev. Lett.* **110**, 135704 (2013).
 - ¹⁸ C. Karrasch and D. Schuricht, Dynamical phase transitions after quenches in nonintegrable models, *Phys. Rev. B* **87**, 195104 (2013).
 - ¹⁹ J. N. Kriel, C. Karrasch, and S. Kehrein, Dynamical quantum phase transitions in the axial next-nearest-neighbor Ising chain, *Phys. Rev. B* **90**, 125106 (2014).
 - ²⁰ M. Heyl, Scaling and Universality at Dynamical Quantum Phase Transitions, *Phys. Rev. Lett.* **115**, 140602 (2015).
 - ²¹ S. Vajna and B. Dóra, Topological classification of dynamical phase transitions, *Phys. Rev. B* **91**, 155127 (2015).
 - ²² M. Schmitt and S. Kehrein, Dynamical quantum phase transitions in the Kitaev honeycomb model, *Phys. Rev. B* **92**, 075114 (2015).
 - ²³ Z. Huang and A. V. Balatsky, Dynamical quantum phase transitions: Role of topological nodes in wave function overlaps, *Phys. Rev. Lett.* **117**, 086802 (2016).
 - ²⁴ A. A. Zvyagin, Dynamical quantum phase transitions (Review Article), *Low Temp. Phys.* **42**, 971-994 (2016).
 - ²⁵ U. Bhattacharya and A. Dutta, Emergent topology and dynamical quantum phase transitions in two-dimensional closed quantum systems, *Phys. Rev. B* **96**, 014302 (2017).
 - ²⁶ S. Bhattacharjee and A. Dutta, Dynamical quantum phase transitions in extended transverse Ising models, *Phys. Rev. B* **97**, 134306 (2018).
 - ²⁷ M. Heyl, Dynamical quantum phase transitions: a review, *Rep. Prog. Phys.* **81** 054001 (2018).
 - ²⁸ B. Zhou, C. Yang, and S. Chen, Signature of a nonequilibrium quantum phase transition in the long-time average of the Loschmidt echo, *Phys. Rev. B* **100**, 184313 (2019).
 - ²⁹ A. L. Corps and A. Relano, Theory of dynamical phase transitions in quantum systems with symmetry-breaking eigenstates, *Phys. Rev. Lett.* **130**, 100402 (2023).
 - ³⁰ H. Cheraghi and N. Sedlmayr, Dynamical quantum phase transitions following double quenches: persistence of the initial state vs dynamical phases, *New J. Phys.* **25**, 103035 (2023).
 - ³¹ B. Zhou, Y. Zeng, and S. Chen, Exact zeros of the Loschmidt echo and quantum speed limit time for the dynamical quantum phase transition in finite-size systems, *Phys. Rev. B* **104**, 094311 (2021).
 - ³² Y. Zeng, B. Zhou, and S. Chen, Dynamical singularity of the rate function for quench dynamics in finite-size quantum systems, *Phys. Rev. B* **107**, 134302 (2023).
 - ³³ C. Yang, L. Li and S. Chen, Dynamical topological invariant after a quantum quench, *Phys. Rev. B* **97**, 060304(R) (2018).
 - ³⁴ D. Liska and V. Gritsev, The Loschmidt Index, *SciPost Phys.* **10**, 100 (2021).
 - ³⁵ C. Y. Wong, T. H. Hui, P. D. Sacramento, and W. C. Yu, Entanglement in quenched extended Su-Schrieffer-Heeger model with anomalous dynamical quantum phase transitions, *Phys. Rev. B* **110**, 054312 (2024).
 - ³⁶ S. Vajna and B. Dóra, Disentangling dynamical phase transitions from equilibrium phase transitions, *Phys. Rev. B* **89**, 161105(R) (2014).
 - ³⁷ F. Andraschko and J. Sirker, Dynamical quantum phase transitions and the Loschmidt echo: A transfer matrix approach, *Phys. Rev. B* **89**, 125120 (2014).
 - ³⁸ S. Sharma, S. Suzuki, and A. Dutta, Quenches and dynamical phase transitions in a nonintegrable quantum Ising model, *Phys. Rev. B* **92**, 104306 (2015).
 - ³⁹ R. Jafari, Dynamical Quantum Phase Transition and Quasi Particle Excitation, *Sci Rep* **9**, 2871 (2019).
 - ⁴⁰ M. Sadrzadeh, R. Jafari, and A. Langari, Dynamical topological quantum phase transitions at criticality, *Phys. Rev. B* **103**, 144305 (2021).
 - ⁴¹ S. Stumper, M. Thoss, and J. Okamoto, Interaction-driven dynamical quantum phase transitions in a strongly correlated bosonic system, *Phys. Rev. Research* **4**, 013002 (2022).
 - ⁴² L. Rossi and F. Dolcini, Nonlinear current and dynamical quantum phase transitions in the flux-quenched Su-Schrieffer-Heeger model, *Phys. Rev. B* **106**, 045410 (2022).
 - ⁴³ U. Divakaran, S. Sharma, and A. Dutta, Tuning the presence of dynamical phase transitions in a generalized XY spin chain, *Phys. Rev. E* **93**, 052133 (2016).
 - ⁴⁴ J. C. Halimeh and V. Zauner-Stauber, Dynamical phase diagram of quantum spin chains with long-range interactions, *Phys. Rev. B* **96**, 134427 (2017).
 - ⁴⁵ V. Zauner-Stauber and J. C. Halimeh, Probing the anomalous dynamical phase in long-range quantum spin chains through Fisher-zero lines, *Phys. Rev. E* **96**, 062118 (2017).
 - ⁴⁶ T. Obuchi, S. Suzuki, and K. Takahashi, Complex semiclassical analysis of the Loschmidt amplitude and dynamical quantum phase transitions, *Phys. Rev. B* **95**, 174305 (2017).
 - ⁴⁷ E. Lieb, T. Schultz, and D. Mattis, Two soluble models of an antiferromagnetic chain, *Ann. Phys. (NY)* **16**, 407 (1961).
 - ⁴⁸ J. E. Bunder and R. H. McKenzie, Effect of disorder on quantum phase transitions in anisotropic XY spin chains in a transverse field, *Phys. Rev. B* **60**, 344 (1999).
 - ⁴⁹ Q. Luo, J. Zhao, and X. Wang, Fidelity susceptibility of the anisotropic XY model: The exact solution, *Phys. Rev. E* **98**, 022106 (2018).